Molecular Crystals and Liquid Crystals

Publication details, including instructions for authors and subscription information:
http://www.tandfonline.com/loi/gmcl20

Morphology of New (P2 1 / n) Metastable Anthracene Modification Crystals, Grown from the Vapor Phase

B. Marciniak [a] , E. Rozycka-Sokolowska [a] & V. Pavlyuk [a]

[a] Institute of Chemistry and Environment Protection, Pedagogical University, Czestochowa, Poland

Version of record first published: 18 Oct 2010

To cite this article: B. Marciniak, E. Rozycka-Sokolowska & V. Pavlyuk (2002): Morphology of New (P2 1 /n) Metastable Anthracene Modification Crystals, Grown from the Vapor Phase, Molecular Crystals and Liquid Crystals, 383:1, 81-97

To link to this article: http://dx.doi.org/10.1080/713738761

Mol. Cryst. Liq. Cryst., Vol. 383, pp. 81–97

1058-725X/02 $12.00 + .00
DOI: 10.1080/10587250290120396

MORPHOLOGY OF NEW ($P2_1/n$) METASTABLE ANTHRACENE MODIFICATION CRYSTALS, GROWN FROM THE VAPOR PHASE

B. Marciniak, E. Rozycka-Sokolowska, and V. Pavlyuk
Institute of Chemistry and Environment Protection, Pedagogical University, Czestochowa, Poland

The morphology of the vapor-grown crystals of a new metastable anthracene modification (that crystallizes in the monoclinic space group $P2_1/n$ with $a = 8.553(2)$, $b = 6.021(1)$, $c = 22.334(4)$ Å, $\beta = 124.54(3)^\circ$, and four molecules per unit cell) was determined from the X-ray single crystal orientation data and optical reflection goniometry measurements. In the standard space group $P2_1/c$, the crystals of this new phase possessed a rhomboidal tabular habit with two major {002} faces oriented in [001] direction, and twelve lateral faces of {11$\bar{3}$}, {111}, {100}, and {102}. This morphology differs nearly fully from that observed for the crystals of a long-known parent anthracene phase ($P2_1/a$) grown under the same conditions. The experimental morphologies of both crystal phases were compared with those predicted from the periodic band chain (PBC) theory of Hartman and Perdok. Moreover, the melting point for this new metastable anthracene phase, equal to 215.1°C, was determined with help of a differential scanning calorimeter.

Keywords: metastable anthracene; crystal morphology; vapor growth

INTRODUCTION

One of the most thoroughly investigated classes of high purity organic crystals is that of rigid aromatic molecules such as simple hydrocarbons like anthracene ($C_{14}H_{10}$). This aromatic hydrocarbon is treated commonly as the arch-type of organic molecular solids; the properties of its crystals are known best in all aspects of crystal physics [1–3].

Received 20, August 2001; accepted 12, March 2002.

We are much indebted to Dr Piotr Bragiel for the DSC measurements and for voluble discussions.

Address correspondence to B. Marciniak, Institute of Chemistry and Environment Protection, Pedagogical University, al. Armii Krajowej 13/15, Czestochowa, 42-201, Poland. E-mail: crystal@cz.onet.pl

Due to extended π-electron systems of constituent molecules, charge carriers and excitons in anthracene crystal can be excited by light in visible or near UV spectral range. This favors its potential applicability as a low-cost photoconductor [4,5]. Moreover, it has found widespread use as scintillation crystal [6,7] because of its short-lived luminescence and near unity quantum yield.

In their papers, Parkinson et al. [8] and Ramdas et al. [9] described the facile production of a triclinic $P\bar{1}$ metastable phase of anthracene, which was discovered from the analysis of the electron diffraction patterns of the thermodynamically stable parent phase ($P2_1/a$) that had suffered stress at room temperature. Apart from this triclinic phase, two monoclinic $P2_1/c$ and $P2_1/n$ phases having similar lattice energies may be expected for anthracene, as it was shown by an "atom-atom" calculation by Craig et al. [10].

The existence of that metastable phase of anthracene, predicted theoretically to crystallize in the monoclinic space group $P2_1/n$ with four molecules per unit cell (Craig et al. [10]) was confirmed experimentally through structure examination of several selected anthracene crystals grown by sublimation [11].

The lattice parameters of this new metastable phase solved and refined from X-ray data, obtained with the help of an automatic DARCH-1 single crystal diffractometer (MoK_α) are: $a = 8.553(2)$, $b = 6.021(1)$, $c = 22.333(4)$ Å, and $\beta = 124.54(3)^\circ$. All carbon and hydrogen atom positions have been determined and refined to $R = 0.044$ for 330 unique reflections.

Although no considerable differences of crystal shape were observed during the selection of samples for crystal structure examinations, further precise X-ray orientation data in combination with the results of the optical reflection goniometry measurements have shown that the crystals of this metastable anthracene phase had faces with forms different from those of the thermodynamically stable monoclinic phase $P2_1/a$.

In this paper we are focusing on experimentally observed morphologies of the vapor grown crystals of the metastable and parent anthracene phases, which were obtained in one growth run under the same conditions of temperature and pressure.

First, we characterize the purity of the starting anthracene, its purification and the growth conditions of the crystals. Then, we report the observed morphologies of both of the anthracene phases' crystals defined by the above X-ray orientation data and by the optical reflection goniometry measurements. Finally, we compare the observed morphologies with those predicted on the basis of the structures of these two phases with the help of the geometrical and attachment energy models based on the periodic band chain (PBC) theory. In order to make this comparison, the

structures of these two anthracene phases were standardized to space group $P2_1/c$.

Moreover, the melting and the freezing temperatures for the metastable anthracene phase were determined from the onsets of the endo- and exothermic peaks recorded with the help of a differential scanning calorimeter.

EXPERIMENTAL

Purity and Purification

The starting material was "analytically pure" anthracene purchased from Naftochem (Gliwice, Poland).

The samples used for the analytical study were prepared from this material by zone refining and further extraction of impurities collected in the upper, central, and bottom parts of the zone-melted ingots. The zone purification was done in the multistage apparatus [12] with the help of 100 zone-melted passages going through the material sealed in the Pyrex glass tubes under pressure of 52 kPa of spectrally pure nitrogen.

Analyses were carried out on a Hewlett-Packard 6890 GC System gas chromatograph equipped with FID detector and with a split/splitless type injector. A fused-silica capillary column, 30 m × 0.32 mm I.D., filled with a HP1 methyl silicone as a stationary phase, was employed. The column was heated at the linear increase of temperature from 70°C to 290°C, with programmed rate of 10°C/min. A split ratio of helium used as a carrier gas to the analyzed samples was 5:1.

For the identification of impurities, a Hewlett-Packard 5890 series II gas chromatograph equipped with mass spectrometry (MS) detector was also used. The composition of chloroform extracts, containing all the contaminants identified in this study, is presented in Table 1.

The commercial anthracene was initially crystallized from dimethylsulfoxide (DMSO) to remove the main impurity carbazole [12], which is difficult to remove by zone refining [13]. After removing trace amounts of DMSO from crystallized anthracene by rinsing them in a stream of hot water, the material was extensively chromatographed on columns filled with SiO_2 and Al_2O_3, and then sublimed under vacuum.

Such prepurified anthracene was extensively zone refined by using a multistage zone refiner as described previously [14] (two-fold passage of 100 molten zones with the rate of 10 mm/h in the first and 5 mm/h in the second stage; and spectrally pure nitrogen as an inert gas). Total impurities content in the final material collected from the central and upper parts of zone-melted ingots was ≤ 0.01 mass%.

TABLE 1 Compositions of Chloroform Extracts of Starting Anthracene (Naftochem, Poland) Obtained from the Upper, Central, and Bottom Parts of the Zone-Melted Ingots

		Components content %		
No.	Component	Zone-melted top	Zone-melted centre	Zone-melted bottom
1	acenaphthene	0.01	<0.01	1.00
2	9H-fluorene	0.01	0.04	0.09
3	9,10-dihydroanthracene	—	—	0.05
4	phenanthrene	<0.01	0.05	0.17
5	anthracene	97.43	94.60	94.40
6	9H-carbazole	2.38	4.18	2.55
7	1-methylanthracene	0.05	0.91	1.22
8	2-methylanthracene	0.06	0.16	0.21
9	9,10-anthracenedion	—	—	0.01
10	1,4-dihydro-1,8-dimethyl-phenanthrene	—	—	0.01
11	pyrene	—	—	0.08
12	phenyldibenzocarbazole	—	0.01	0.20
	remain	0.05	0.04	0.01

Crystal Growth

The crystals of the thermodynamically stable parent ($P2_1/a$) and metastable ($P2_1/n$) anthracene phases were obtained from the vapor phase using the plate sublimation technique, described in the previous paper [11].

The crystals were grown simultaneously under a stable 2.5×10^{-2} mbar vacuum and at the constant temperature of the source material of 93°C with the rate of ca 1.44×10^{-2} mg/h on spontaneously formed seeds.

On the basis of crystal structures of both phases of crystals determined on a DARCH 1 single crystal diffractometer (MoK_α radiation) [11], the contribution of the metastable modification crystals in their whole population grown in one growth run was established as a no more than 5%.

Morphology Studies

The morphology of the crystals grown by the above technique was examined using a DRON 3.0 powder diffractometer (CuK_α radiation) with a computer registration of profile reflex, and a Carl Zeiss ZRG-2 optical reflection goniometer that was used for their orientation and the measurement of the interfacial angles, respectively.

To recognize the crystals of both anthracene phases, the X-ray diffraction data collected with the help of the above-mentioned DARCH 1 single

crystal diffractometer were used. Such a recognition method is rather strenuous and time consuming; however, due to high precision of crystal structure determination we could select crystals of the metastable modification without any doubts. As it was shown in the previous paper [11], the powder diffraction method, which was simpler to use, proved to be not sensitive enough for the detection of this metastable structure.

The crystals used for morphology studies were selected from those grown with only a small face in contact with the support (cooper plate). Similar to Karl's observation [5], such grown crystals were most perfect and they came off from this plate very easily, without any damages to their external habit.

Differential Scanning Calorimetry Measurement

Differential Scanning Calorimetry (DSC) measurements of crystal samples of the parent and metastable anthracene phases selected on the basis of the X-ray crystal structure data were carried out with the help of a Simultaneous Thermal Analyzer (NETZSCH STA 409C) in a flowing argon atmosphere. The samples were placed in tightly closed crucible pots made from aluminum; the same empty crucible pot was used as a reference. Measurements of both crystal samples were conducted in the temperature range from 20°C to 240°C, with the programmed heating rate of 10°C/min. The melted samples were then cooled in the same temperature range. The DSC analyzer used was calibrated previously with the help of five pure metals taken from a NETZSCH calibration kit.

RESULTS AND DISCUSSION

Experimental Morphology

All the crystals of anthracene grown in this study possessed a rhomboidal tabular habit with small lateral faces, irrespective of their structure. The largest crystals of the stable, parent phase ($P2_1/a$) were ca $8 \times 8 \times 3\,mm^3$ while those of the metastable modification ($P2_1/n$) had somewhat smaller dimensions of ca. $5 \times 5 \times 2\,mm^3$. A typical grown crystal of the metastable anthracene phase is shown in Figure 1.

The crystallographic orientation data determined from the single crystal diffraction patterns have shown that the growth direction of the two parallel largest faces present in the crystals of the $P2_1/n$ and $P2_1/a$ anthracene phases is [00l]. As an example, a typical X-ray diffraction pattern registered for a crystal of the metastable anthracene phase is presented in Figure 2. The intensities ratio of the type reflections with $l = 2n$ is $I_{0\ 0\ 2}$:$I_{0\ 0\ 4}$:$I_{0\ 0\ 6}$:$I_{0\ 0\ 8}$:$I_{0\ 0\ 10}$ = 1000:240:50:30:10.

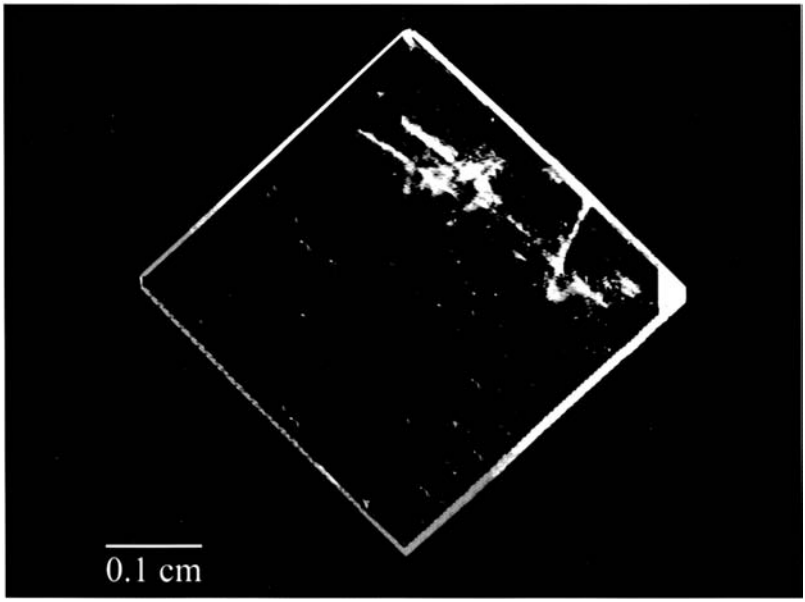

FIGURE 1 Photograph of a typical crystal of the $P2_1/n$ metastable anthracene modification grown from the vapor phase.

The observed morphologies of crystals of both types of phases drawn with the help of the computer program SHAPE [15] are shown in Figure 3. The drawings presented in this figure illustrate an external habit of these crystals in the standard space group $P2_1/c$. The STRUCTURE TIDY program [16] was used to transform the $P2_1/a$ and $P2_1/n$ space groups to the space group of $P2_1/c$. The standardized atomic positional parameters and unit cells dimensions in the $P2_1/c$ space group are given in Table 2. The above-mentioned Figure 2 also illustrates the interrelations between the unit cells in the $P2_1/a$ and $P2_1/n$ space groups and between the cells in the standard space group of $P2_1/c$. Considering the forms present in the parent anthracene crystals grown, i.e., the {001} form containing the two major (001) and (00$\bar{1}$) faces and the forms of {11$\bar{1}$}, {110}, and {20$\bar{1}$} containing ten lateral faces, it may be noted that the morphology of the crystals is the same as that observed by Sloan et al. [17]. The above forms correspond, respectively, to the major form of {100} and the {01$\bar{1}$}, {11$\bar{1}$}, and {10$\bar{2}$} lateral forms in the $P2_1/c$ space group given in Table 3. In case of the metastable anthracene crystals, the fourteen observed faces which formed five different forms listed in this table correspond to the two major (002) and (00$\bar{2}$) faces and to the twelve lateral faces forming the {10$\bar{1}$}, {101}, {110}, and {11$\bar{4}$} forms in the $P2_1/n$ space group. Although

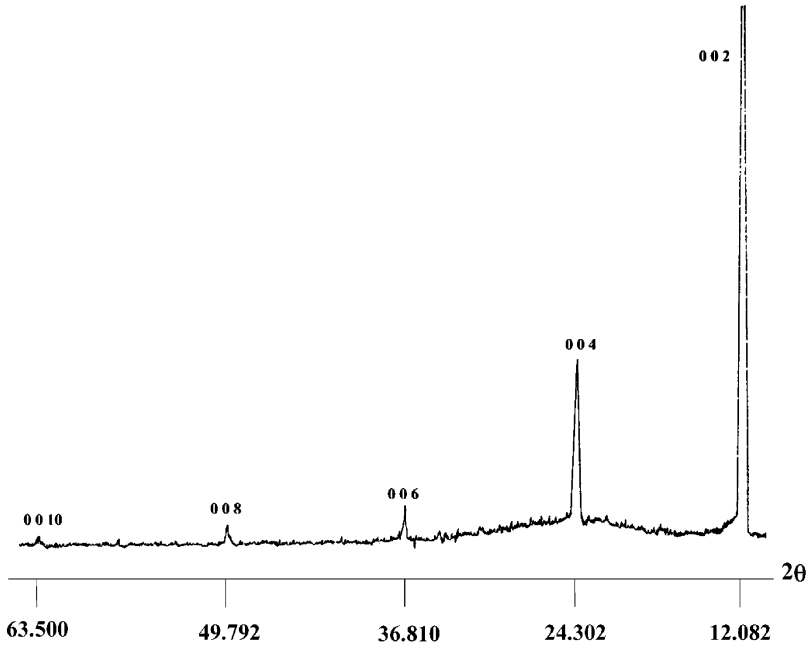

FIGURE 2 X-ray diffraction pattern for a crystal of the metastable phase of anthracene.

the grown crystals of the parent and metastable anthracene phases do not significantly differ in the habit, they exhibit nearly full difference in the forms. As one can notice from the comparison of the morphologies presented in Figures 2a and 2b ($P2_1/c$ space group), out of the twelve observed faces in the parent anthracene crystals that form four of the above-mentioned forms of {100}, {01$\bar{1}$}, {11$\bar{1}$}, and {10$\bar{2}$}, only the {100} form also occurs in the crystals of the metastable anthracene modification. Such a large difference in forms indicates that the morphology of freely grown anthracene crystals may be treated not only as an indicative but also, to a large extent, as conclusive evidence of its polymorphism, comprised of the $P2_1/a$ stable parent phase and its $P2_1/n$ metastable modification.

Modelling Crystal Morphology

Morphological modelling techniques are based on correlating the bulk structure with the external crystal morphology. A satisfying description of the morphology may be obtained by means of the geometrical and

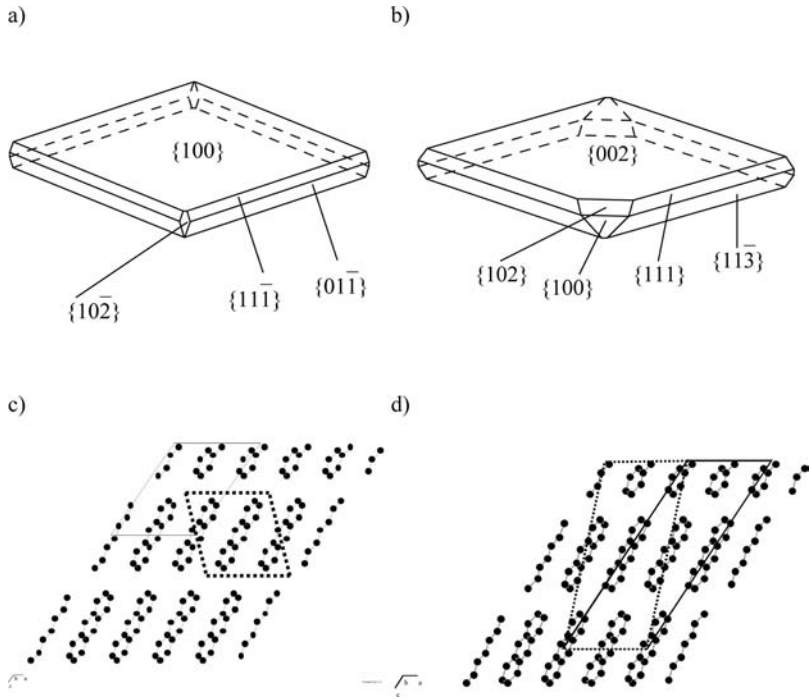

FIGURE 3 Experimental morphologies of grown crystals of the parent (a) and metastable (b) phases of anthracene in the standard space group $P2_1/c$; representation of the packing of anthracene molecules and the interrelations between unit cells in the $P2_1/a$ and $P2_1/c$ (c), and $P2_1/n$ and $P2_1/c$ (d) space groups. The unit cells in the $P2_1/a$ and $P2_1/n$, and $P2_1/c$ space groups are denoted by the solid line and the dashed line, respectively.

attachment energy models, based on Bravais-Friedel-Donnay-Harker (BFDH) law [18–20] and on the Hartman-Perdok (HP) [21] theory of PBC, respectively. These two models are founded on the assumptions that the growth rate R of a face (hkl) is related to close-packing and interlayer spacing d_{hkl} of the molecular planes in different crystallographic directions ($R \propto 1/d_{hkl}$) and to the attachment energy (E_{att}) of the molecule in the surface ($R \propto E_{att}$), respectively. Due to weak van der Waals's intermolecular interactions which generally occur in molecular crystals, predictions of their growth morphology based on crystal structure prove to be quite successful. The computer program HABIT [22,23] used in this study is one of the most convenient methods among many other computer methods [24] used for determining periodic chains of strong bonds, which define a flat (F) face (hkl) as that containing at least two PBCs in the growth slice of

TABLE 2 Unit Cell Dimensions and Atomic Positional Parameters for Crystals of the Parent and Metastable Phases of Anthracene in $P2_1/a$ and $P2_1/n$ Space Groups, respectively, and in Standard Space Group $P2_1/c$

Parent anthracene phase

Unit cell in $P2_1/a$ [26]: $a = 8.562$, $b = 6.038$, $c = 11.184$ Å, $\beta = 124.42°$					Unit cell in $P2_1/c$: $a = 9.4582$, $b = 6.0158$, $c = 8.5526$ Å, $\beta = 103.508°$				
Atoms		x	y	z	Atoms		x	y	z
H1	4(e)	0.12700	0.08200	0.45900	H1	4(e)	0.04100	0.08200	0.16800
H5	4(e)	−0.02700	−0.27100	0.38000	H2	4(e)	0.12000	0.72900	0.09300
C1	4(e)	0.08670	0.02880	0.36440	C1	4(e)	0.13560	0.02880	0.22230
C7	4(e)	−0.00350	−0.18060	0.31560	C2	4(e)	0.18440	0.81940	0.18090
H2	4(e)	0.18200	0.29700	0.31300	H3	4(e)	0.18700	0.29700	0.36900
C2	4(e)	0.11780	0.15550	0.27980	C3	4(e)	0.22020	0.15550	0.33800
C3	4(e)	0.05890	0.08170	0.13840	C4	4(e)	0.36160	0.08170	0.42050
H3	4(e)	0.15100	0.35000	0.08200	H4	4(e)	0.41800	0.15000	0.06900
C4	4(e)	0.08750	0.20740	0.04770	C5	4(e)	0.45230	0.29260	0.03980
C5	4(e)	−0.03030	−0.13140	0.08960	C6	4(e)	0.58960	0.36860	0.11990
H4	4(e)	−0.12300	−0.40500	0.14700	H5	4(e)	0.64700	0.09500	0.27000
C6	4(e)	−0.06010	−0.25770	0.18300	C7	4(e)	0.68300	0.24230	0.24310

Metastable anthracene modification

Unit cell in $P2_1/n$ [11]: $a = 8.553(2)$, $b = 6.021(1)$, $c = 22.333(4)$ Å, $\beta = 124.54(3)°$					Unit cell in $P2_1/c$: $a = 8.5530$, $b = 6.0210$, $c = 18.8498$ Å, $\beta = 102.592°$				
Atoms		x	y	z	Atoms		x	y	z
C3A	4(e)	0.0540(4)	0.0770(5)	0.0720(18)	C1	4(e)	0.01831	0.57696	0.42796
H2A	4(e)	0.2080(19)	0.2500(2)	0.1850(8)	H1	4(e)	0.02334	0.25412	0.18498
C2A	4(e)	0.1050(3)	0.1590(4)	0.1365(15)	C2	4(e)	0.03156	0.65850	0.36350
C4A	4(e)	0.0880(3)	0.2040(4)	0.0230(2)	C3	4(e)	0.06524	0.20406	0.02256
C5A	4(e)	0.0340(3)	0.1230(5)	0.9520(2)	C4	4(e)	0.08216	0.37699	0.45211
C1A	4(e)	0.0920(5)	0.0390(6)	0.1840(3)	C5	4(e)	0.09257	0.53945	0.31549
H1A	4(e)	0.1300(2)	0.0200(3)	0.2360(10)	H2	4(e)	0.10078	0.52302	0.26408
H4A	4(e)	0.1000(2)	0.3100(3)	−0.0030(8)	H3	4(e)	0.10138	0.18545	0.49722
C6A	4(e)	0.0610(4)	0.2560(4)	0.9060(2)	C6	4(e)	0.15456	0.24414	0.40647
C7A	4(e)	0.0110(3)	0.1810(5)	0.8430(17)	C7	4(e)	0.16757	0.31898	0.34295
H7A	4(e)	1.0200(3)	0.3200(3)	0.8100(11)	H4	4(e)	0.21042	0.17512	0.30958
H6A	4(e)	0.1560(19)	0.3900(3)	0.9080(8)	H5	4(e)	0.24808	0.11108	0.40800
H5B	4(e)	0.3650(10)	0.9260(14)	0.0680(4)	H6	4(e)	0.29719	0.57416	0.56802
C4B	4(e)	0.5840(3)	0.4760(4)	0.1797(15)	C8	4(e)	0.40460	0.47590	0.17971
H4B	4(e)	0.6300(2)	0.4300(3)	0.2210(11)	H7	4(e)	0.40729	0.43075	0.22149
C6B	4(e)	0.3650(3)	0.6530(5)	0.8584(15)	C9	4(e)	0.49331	0.34747	0.14155
C1B	4(e)	0.4370(3)	0.5840(4)	0.9320(9)	C10	4(e)	0.49507	0.41555	0.06801
H6B	4(e)	0.3070(10)	0.8040(13)	0.8500(4)	H8	4(e)	0.54286	0.19571	0.14986
C7B	4(e)	0.5900(3)	0.2880(5)	0.0246(13)	C11	4(e)	0.56529	0.28829	0.02459
C2B	4(e)	0.5270(3)	0.3560(4)	0.9568(11)	C12	4(e)	0.57034	0.14369	0.45678
H7B	4(e)	0.6440(14)	0.1100(2)	0.0500(6)	H9	4(e)	0.59339	0.10938	0.05031
C5B	4(e)	0.4430(3)	0.7570(4)	0.0910(2)	C13	4(e)	0.64783	0.25688	0.40869
C3B	4(e)	0.5070(4)	0.6750(7)	0.1604(19)	C14	4(e)	0.65316	0.17518	0.33955
H3B	4(e)	0.4500(4)	0.7800(5)	0.1870(17)	H10	4(e)	0.73362	0.28243	0.31347

TABLE 3 Reciprocal of Interplanar Spacing ($1/d_{hkl}$), Attachment Energy ($|E_{att}|$), and Morphological Importance of Faces (MI) Calculated for Crystals of the Parent and Metastable Phases of Anthracene in the Standard Space Group $P2_1/c$

	DH model		HP model	
Form	1/dhkl ($Å^{-1}$)	MI	$\|E_{att}\|$ (kcal/mol)	MI
Parent anthracene phase				
{100}*	0.109	1	6.35	1
{01$\bar{1}$}*	0.205	2	16.52	3
{11$\bar{1}$}*	0.219	3	16.08	2
{10$\bar{2}$}*	0.240	4	17.86	4
{002}	0.241	5	20.56	9
{1$\bar{1}$1}	0.245	6	18.77	6
{2$\bar{1}$1}	0.278	7	18.73	5
{20$\bar{2}$}	0.284	8	20.02	8
{102}	0.286	9	21.25	10
{2$\bar{1}$1}	0.319	10	19.00	7
{020}	0.332	11	24.11	13
{1$\bar{2}$0}	0.350	12	23.89	12
{202}	0.360	13	21.39	11
Metastable anthracene modification				
{002}*	0.109	1	5.79	1
{100}*	0.120	2	9.00	3
{10$\bar{2}$}	0.143	3	9.14	4
{01$\bar{1}$}	0.175	4	11.29	5
{102}*	0.178	5	8.73	2
{1$\bar{1}$1}	0.205	6	15.57	8
{111}*	0.218	7	15.11	7
{01$\bar{3}$}	0.233	8	13.94	6
{200}	0.240	9	16.84	9
{20$\bar{2}$}	0.241	10	18.95	13
{11$\bar{3}$}*	0.245	11	17.53	11
{1$\bar{1}$3}	0.278	12	17.48	10
{202}	0.284	13	18.39	12

*The forms observed experimentally.

thickness d_{hkl}. Using this program and the atom-atom method to sum all the significant intermolecular forces interacting with a defined central molecule, the crystal lattice energies equating the sublimation enthalpy ΔH_{sub} were calculated for the parent and metastable anthracene phases from the crystal structure data determined by Mason [25] and by Marciniak and Pavlyuk [11], respectively. Figure 4 illustrates the results of the lattice energy calculations as a function of a summation limit, obtained for some potentials tested in this study such as those given by Williams [26], Momany

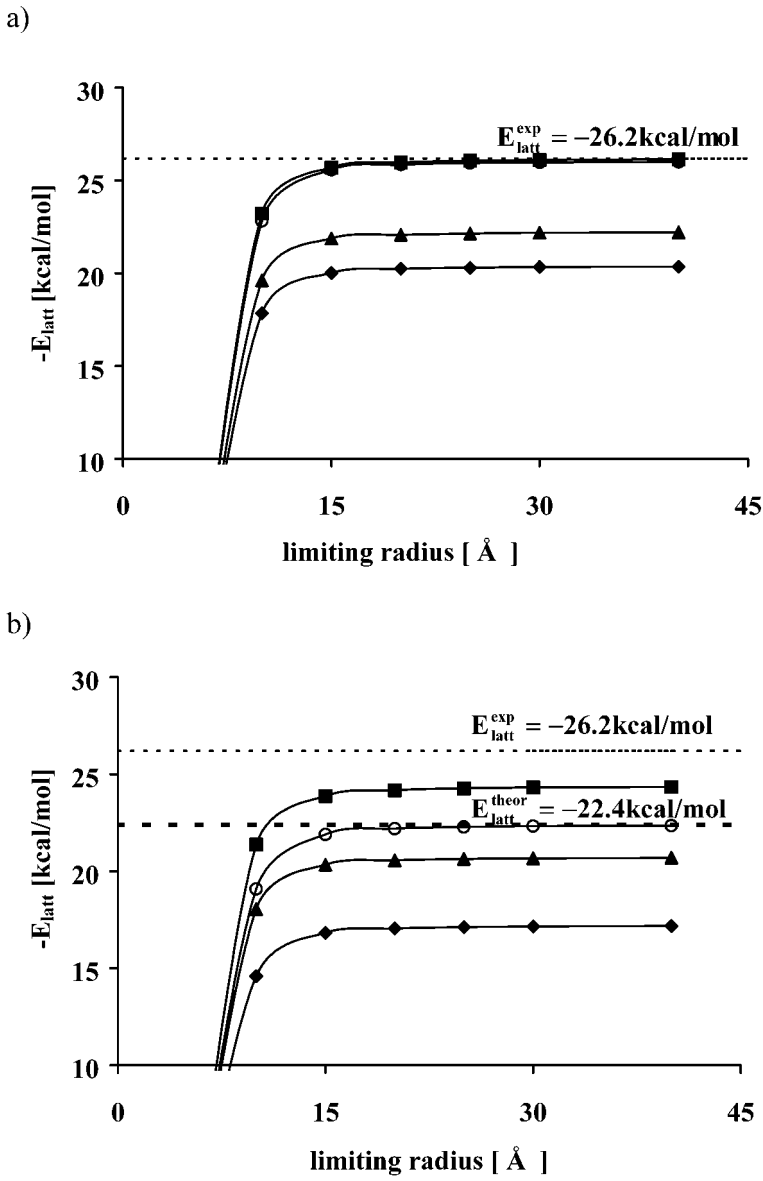

FIGURE 4 Lattice energy as a function of a summation limit calculated for the parent (a) and metastable (b) phases of anthracene with the help of the Momany et al.'s (◆), Williams's (■), Govers's (▲), and Nèmethy et al.'s (○) potential functions. The "experimental" lattice energy and that calculated by Craig et al. are denoted by the thin and thick dashed lines, respectively.

et al. [27], Govers [28], and Nemethy et al. [29]. The lattice energy of −26.13 kcal/mol calculated for the parent phase with the help of the former potential (Figure 4a) is nearly equal to the "experimental" lattice energy (E_{latt}^{exp}) of anthracene, i.e., −26.2 kcal/mol [30] ($E_{latt}^{exp} = -\Delta H_{sub} - 2RT$, where 2RT represents a correction factor for the difference between the gas phase enthalpy and the vibrational contribution to the crystal enthalpy [26]). In the case of the metastable anthracene modification, Williams's potential yielded the lattice energy of −24.34 kcal/mol, which is 1.86 kcal/mol larger than the above "experimental" value (Figure 4b). As one can notice from this figure, a significantly better agreement could be achieved when the value of −22.40 kcal/mol predicted theoretically for the $P2_1/n$ anthracene modification by Craig et al. [10] and the potential given by Nemethy et al. [29] were used. However, any significant differences in the morphologies of the $P2_1/n$ anthracene phase crystals predicted by HABIT with the use of Williams's or Nemethy et al.'s potentials were not observed.

The reciprocal of the interplanar spacings ($1/d_{hkl}$) resulted from the BFDH model, according to which the most important morphological forms in crystals of the parent and metastable anthracene phases (after standardization of their structures) were identified. Moreover, the attachment energies (E_{att}) calculated for the above BFDH forms from the HP model are listed in Table 3.

Although both sets of the parameters obtained show that the two models used predict generally all the faces present in the crystals of the parent and metastable phases of anthracene, in the latter crystals only the {002} and {100} forms predicted by BFDH model and the forms of {002}, {100}, and {102} predicted by the HP model occur in the external morphologies constructed with the help of the Dowty's program SHAPE [15] (Figures 4c and 4d, respectively). The parameters also indicate that the {100} form in the parent and the {002} form in the metastable phase crystals should be dominant in their morphologies. The drawings shown in Figures 3a and 3b fully confirm these prediction results.

For the more detailed estimation of the results obtained for the crystals of the metastable anthracene phase, it may also be noticed that the models used significantly underestimate the observed {111} and $\{11\bar{3}\}$ forms (the form $\{11\bar{3}\}$ in particular), giving them considerably lower morphological importance MI (i.e., 7 and 11, respectively; see Table 3) in comparison with their real MI resulting from the relative dimensions of these faces (Figure 2b). At the same time, they overestimate the MI of the {100} and {102} forms observed in the crystals of this metastable phase.

Moreover, in this estimation, it should also be taken into account that the attachment energy ($|E_{att}|$) obtained for the {111} form is higher than the $|E_{att}|$ calculated for the forms of $\{10\bar{2}\}$, $\{01\bar{1}\}$, and $\{01\bar{3}\}$ (Table 3). In case of the $\{11\bar{3}\}$ form observed in the crystals of this metastable phase, apart from

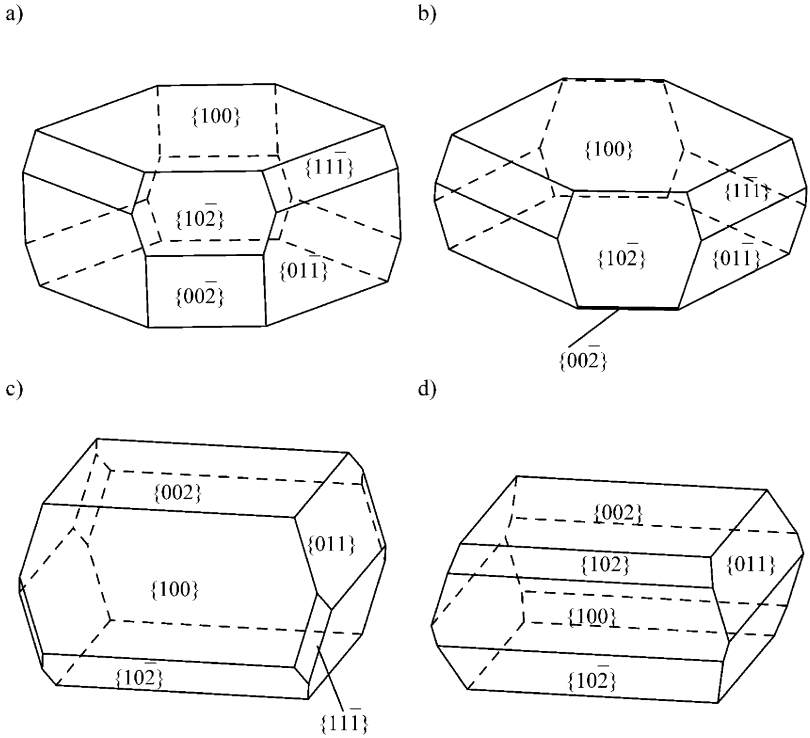

FIGURE 5 Theoretical morphologies of the parent (a and b) and metastable (c and d) anthracene modification crystals, predicted, respectively, by the BFDH and HP models.

these latter forms the three additional ones such as $\{1\bar{1}\bar{1}\}$, {200}, and $\{1\bar{1}3\}$ have lower values of $|E_{att}|$.

In spite of these prediction results, these 6 forms have never been observed in the real crystals of this anthracene phase grown in this study.

In case of parent anthracene crystals, the morphological importance of the observed faces agrees with that predicted by both theoretical models used (Table 3, Figure 2a, and Figures 4a and 4b).

DSC Results

In accordance with McCrone [31], a polymorph is defined as "a solid crystalline phase of a given compound resulting from the possibility of at least two crystalline arrangements of the molecules of that compound in the solid state." Thus, the different polymorphs have different structures,

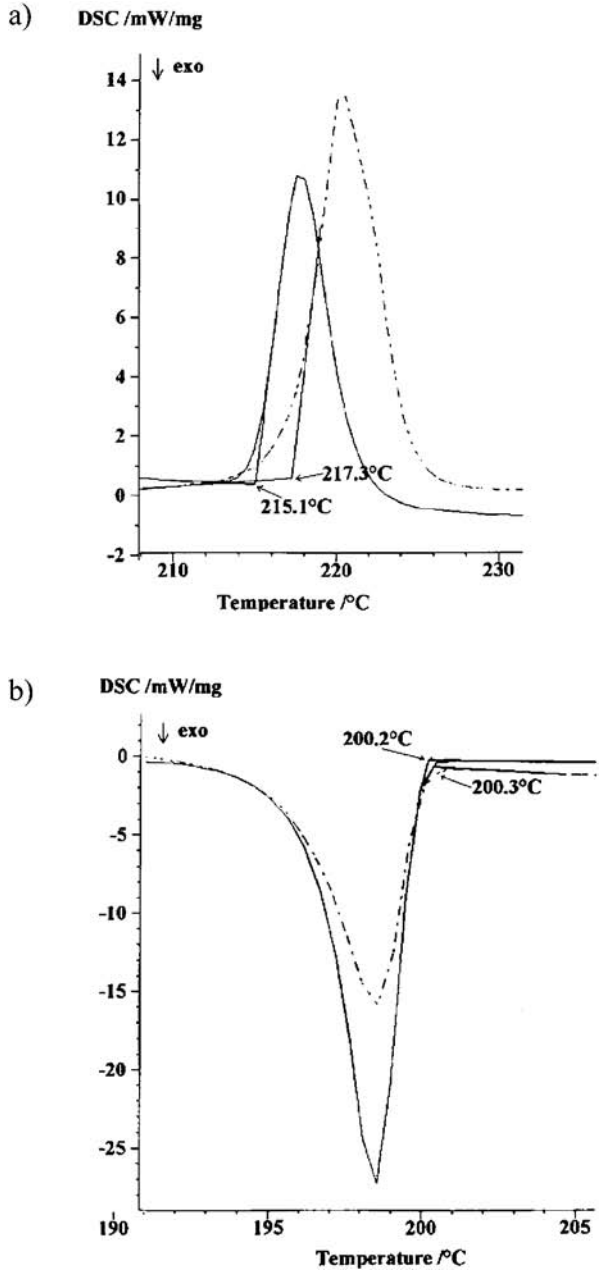

FIGURE 6 The endothermic (a) and exothermic (b) peaks of the parent (solid line) and metastable (dashed line) anthracene phases recorded by DSC method.

and each of them may be treated as a unique material with its own physical and chemical properties. Still, apart from the thermomicroscopic examination with help of the hot-stage polarizing microscope [32–34], which is one of the best methods for the recognition of the polymorphs, some of the other physical measurements, for example, refraction index, melting behavior, IR, and NMR, were also used for this purpose [35].

In order to characterize the melting behavior of anthracene crystals grown in this study, and especially to check if the melting point of its parent phase differs from that of the metastable one, the differential scanning calorimetry measurements were carried out, as was mentioned in a previous section of this article.

The DSC curves recorded during the heating of crystal samples and during the cooling of their melts are shown in Figures 6a and 6b, respectively.

As one can notice from Figure 6a, the melting temperatures determined for the both measured crystal samples as the onset of the endothermic peaks recorded for them are 215.1°C for the metastable and 217.3°C for the parent phase of anthracene. The freezing temperatures determined as the onsets of the exothermic peaks (Figure 6b) resulting from the cooling of the melted samples turned out to be practically the same; within the measurement error—they are 200.2°C and 200.3°C for the parent and metastable phases, respectively.

Such inconsiderable difference in the freezing temperatures of these two phases practically eliminates the possibility of the impurities' influence on their determined melting temperatures.

CONCLUSIONS

As was mentioned in a previous paper [11], at the present stage of our study we assume that the excessive stress and mechanical deformations resulting from a relatively fast growth were the main reasons of the occurrence of the $P2_1/n$ metastable anthracene phase crystals in the population of the sublimed crystals, obtained under the same conditions of temperature and pressure. This assumption is very probable as, according to the prediction of Craig et al., the lattice energy of this phase, which equals −22.40 kcal/mol, is nearer to that predicted for the parent phase (−23.73 kcal/mol) than in case of the $P\bar{1}$ triclinic anthracene modification (−21.31 kcal/mol), whose facile production was observed by Ramdas et al. [9]. An additional argument, supporting the above assumption, is that the same practically freezing points of the $P2_1/n$ phase and the $P2_1/a$ parent phase, which equals 200.2 and 200.3°C, respectively (see Figure 6b), eliminate the possibility of the impurity effect.

In the standard $P2_1/c$ space group, the grown tabular crystals of the metastable anthracene phase containing two major {002} faces (oriented in the [001] direction) and twelve lateral faces of $\{11\bar{3}\}$, {111}, {100}, and {102} exhibit nearly full difference in morphology in relation to the parent anthracene crystals grown under the same conditions. . Only the {100} form present in the $P2_1/n$ phase crystals also occurs in the crystals of the parent anthracene phase, which contain 10 other faces forming the $\{01\bar{1}\}$, $\{11\bar{1}\}$, and $\{10\bar{2}\}$ forms apart from the {100} form. Such a large difference in forms indicates that the morphology of the freely grown crystals of the $P2_1/n$ metastable anthracene phase may be treated as practically conclusive evidence of their existence.

All the faces observed in crystals of both types of anthracene phases can be predicted with the help of the BFDH geometrical and HP attachment energy models. It was found, however, that these prediction results are less accurate in case of the metastable phase. As lower precision of these results could be connected with the lattice energy (see Figure 4b) taken for prediction of the morphology of this phase crystals, we are going to determine the experimental value of this energy.

The DSC results obtained for crystal samples of the both investigated phases lead to the conclusion that the melting temperature of the metastable phase, which has a value of 215.1°C, is distinctly lower than the melting point of the parent anthracene (217.3°C) (both temperatures were determined under the same experimental conditions), may be treated as a convenient parameter enabling recognition of the existence of this new metastable anthracene modification.

REFERENCES

[1] E. A. Silinsh, *Organic Molecular Crystals* (Springer-Verlag, Berlin, 1980).
[2] K. Kojima, *Prog. Cryst. Growth and Charact.*, **23**, 369–420 (1991).
[3] H. Bässler, Semiconducting and photoconducting organic solids, in *Organic Molecular Solids Properties and Applications*, ed. W. Jones (CRC Press Inc., Boca Raton, New York, 1997), Chap. 9, pp. 267–308.
[4] W. Warta, R. Stehle, and N. Karl, *Appl. Phys.*, **A36**, 163–170 (1985).
[5] N. Karl, High purity organic molecular crystals, in *Crystals Growth, Properties, and Applications*, ed. H. C. Freyhardt (Springer-Verlag, Berlin, Heidelberg, New York, 1980), Vol. 4, pp. 1–100.
[6] J. B. Bricks, Scintillations in organic solids, in *Physics and Chemistry of the Organic Solid State*, eds. D. Fox, M. M. Labes, and A. Weissberger (Interscience Publishers, New York, London, Sydney, 1965), Vol. II, pp. 433–508.
[7] L. Papadopoulos, *Nucl. Instr. and Meth.*, **A434**, 337–344 (1999).
[8] G. M. Parkinson, M. J. Goringe, S. Ramdas, J. O. Williams, and J. M. Thomas, *JSC Chem. Commun.*, **134** (1978).
[9] S. Ramdas, G. M. Parkinson, J. M. Thomas, C. M. Gramaccioli, G. Filipini, M. Simonetta, and M. J. Goringe, *Nature*, **284**, 153–154 (1980).

[10] D. P. Craig, J. F. Ogilvie, and P. A. Reynolds, *J. Chem. Soc. Faraday Trans., II,* **72**, 1603–1612 (1976).
[11] B. Marciniak and V. Pavlyuk, *Mol. Cryst. Liq. Cryst.* **373**, 237–250 (2002).
[12] B. Marciniak, *Mol. Cryst. Liq. Cryst.,* **162B**, 301–313 (1988).
[13] G. J. Sloan, *Mol. Cryst. Liq. Cryst.,* **1**, 161–194 (1966).
[14] B. Marciniak, A novel multistage zone refiner for purification of organic materials, in *Solid State Crystals: Growth and Characterization Materials Science and Applications*, eds. J. Zmija, A. Rogalski, and J. Zielinski, *Proc. SPIE*, **3178**, 68–70 (1997).
[15] E. Dowty, *Am. Mineral.*, **65**, 465 (1980).
[16] E. Parthé, K. Cenzual, and R. Gladyshevskii, *J. Alloys Comp.*, **197**, 291–301 (1993).
[17] G. J. Sloan, J. M. Thomas, and J. O. Williams, *Mol. Cryst. Liq. Cryst.*, **30**, 167–174 (1975).
[18] A. Bravais, *Etudes Crystallographiques*, Paris, 1913.
[19] G. Friedel, *Leçon de Cristallographie* (Hermann, Paris, 1911).
[20] J. D. H. Donnay and D. Harker, *Am. Mineralogist*, **22**, 463 (1937).
[21] P. Hartman and W. G. Perdok, *Acta Cryst.*, **8**, 49–52 (1955).
[22] G. Clydesdale, R. Docherty, and K. J. Roberts, *Comput. Phys. Commun.*, **64**, 311–328 (1991).
[23] G. Clydesdale, K. J. Roberts, and R. Docherty, *J. Cryst. Growth,* **166**, 78–83 (1996).
[24] P. Hartman, Modern PBC Theory, in *Morphology of Crystals Part A*, ed. I. Sunagawa (Terra Scientific Publishing Company (TERRAPUB), Tokyo, 1987) pp. 269–319.
[25] R. Mason, *Acta Cryst.*, **17**, 547–554 (1964).
[26] D. E. Williams, *J. Chem. Phys.*, **45**, 3370–3378 (1966).
[27] F. A. Momany, L. M. Carruthers, R. F. McGuire, and H. A. Scheraga, *J. Phys. Chem.*, **78**, 1595–1619 (1974).
[28] H. A. J. Govers, *Acta Cryst.*, **A34**, 960–965 (1978).
[29] G. Nemethy, M. S. Pottle, and H. A. Scheraga, *J. Phys. Chem.*, **87**, 1883–1887 (1983).
[30] R. Docherty, G. Clydesdale, K. J. Roberts, and P. Bennema, *J. Phys. D: Appl. Phys.*, **24**, 89–99 (1991).
[31] W. C. McCrone, Polymorphism, in *Physics and Chemistry of the Organic Solid State*, Vol. 2, eds. D. Fox, M. M. Labes, and A. Weissberger (Interscience, New York, 1965) pp. 725–767.
[32] L. Kofler and A. Kofler, *Thermo-mikro-methoden zur Kennzeichnung organischer Stoffe und Stoffgemische* (Wagner, Innsbruck, 1954).
[33] W. C. McCrone, *Fusion Methods in Chemical Microscopy* (Interscience, New York, 1957).
[34] M. Kuhnert-Brandstätter, *Thermomicroscopy in the Analysis of Pharmaceuticals* (Pergamon, Oxford, 1971).
[35] J. Bernstein, R. J. Davey, and J.-O. Henck, Angew. *Chem. Int. Ed.*, **38**, 3440–3461 (1999).